

An Analysis Of Rc Interior Connection Through Ferrous Steel Plate Coupler

A. ANBUCHEZIAN , M.VAIRAVEL

Principal & professor , Department of Civil Engineering , AnnaPoorana Engineering College , Sankari Main Road Periya Seeragapadi, Salem, Tamil Nadu 636308.

Associate professor, Department of Civil Engineering , AnnaPoorana Engineering College , Sankari Main Road Periya Seeragapadi, Salem, Tamil Nadu 636308

Abstract

This research's assessment process was carried out on the Ferrous steel plate coupler, which has been subjected to the interior column-joint. Almost six specimens have been selected in this process, and the joint test is done using a reversible cyclic-load segment. To showcase the efficiency of the Ferrous steel plate coupler, three types of joints have been considered. The joints used for the process are E-SMRJ, E-OMRJ, and E-FTJ. The third joint used for this process has 0 joint stirrups and no anchorage. This process's outcome proved that specimen one with a Ferrous steel plate coupler has more efficiency than the other specimens. The comparative study in this research is done within the requirements of national codes and the internal codes. The outcome of comparative study shows that the proposed joint specimen's code is excellent, and the prediction made on the shear strength of the joint was very close to the experimentation outcome.

Keywords:Ferrous steel plate coupler, RC, joint strength, joint core, shear strength, flexibility.

Introduction

Beam-column joint (joint) are vulnerable zone and during strong ground motion, the huge amount of shear force always present in this region and amount of this force always higher than the that of adjacent elements such as beams and columns. Absence of studying the shear force in the joint region may result in serious damages or collapse in the structural joint. The main three factors affecting the overall behavior of the joint and these factors are the type of anchorage given to beam main bar, the compressive strength of concrete and shear strength joint.

Mostofinejad & Akhlaghi, 2017a) have been reported that the behavior of the ten numbers of RC high strength interior joint with cyclic loading condition. From the detailed study, they have concluded that the joint area is mainly affected by the grade of concrete and lateral ties or spiral.

Halahla et al., 2019) have been reported that the importance of concrete strength and prove this a database has been constructed and categories the database based on the types of joint and failure mode of the joint. Their study concluded that the shear capacity of the joint is greatly affected by concrete compressive strength. Many researchers have reported the importance of hoop reinforcement in column, beam and joint region to improve the strength and ductility.

Marimuthu & Kothandaraman, n.d. have been reported that the importance of 'joint aspect ratio', shear index and column axial stress in the interior joint by conducting an experimental study. From the experimental study, they have concluded that the shear capacity of the interior joint is mainly affected by 'joint aspect ratio' and shear index.

Mahmud et al., 2018 have been conducted that the test on 43 interior joints under the seismic condition and their study concluded that the shear strength of the interior joint was greatly improved by adding the shear reinforcement in the joint region.

Foorginezhad et al., 2020 has been reported that the behavior four half scaled interior joint specimen and the main investigation parameter was joint shear stress, anchorage length and column depth. From the test results, they found that anchorage 24 times of the diameter of the bar is required to achieve the ultimate strength and anchorage 28 times of the diameter of bar exhibits good energy dissipation capacity.

Chetchotisak et al., 2020; Tingjin et al., 2021 have been investigated that twelve number of interior joint with different reinforcement detailing. From the results of the study, they concluded that the specimen combination of ACI standard hook and full anchorage with hairclip exhibits superior energy dissipation and better hysteretic performance. In brief, the above literature study it has been identified that the shear capacity of the joint is greatly affected by concrete strength, amount of hoop reinforcement and type of anchorage of beam main bar. Many researchers were suggested different joint reinforcement patterns and techniques improve the shear capacity of joint. The joint reinforcement patterns and techniques are spiral reinforcement technique

Annadurai & Ravichandran, 2018, Core reinforcement technique

Wang, 2021 combination of headed bar and hair clip reinforcement technique (Pantelides et al., 2017) square spiral reinforcement inclined bar technique (Abdelwahed, 2019) fibre reinforced technique (Hwang & Park, 2020)[12] and retrofitting technique (Mostofinejad & Akhlaghi, 2017b) The author critically reviewed and listed out the salient features of all the above technique. To overcome the existing construction difficulties in the joint, an innovative technique "Ferrous Steel Plate Coupler bar" has been introduced in the core joint as an alternate option for the standard ninety-degree hook. The results of the experiments showed that the proposed 'steel flat coupler joint' specimen performed very well and especially the ductile behavior was excellent than that of all other specimens. The main important features of the proposed techniques are easy installation, reduced the cost, less time and less usage of labor, manpower and machinery etc., Also, the author have been reported the effect of cost and time of proposed Ferrous Steel Plate Coupler bar joint and their cost and time study concluded that the cost and time consuming for construction using this technique is reduced.

1. RESEARCH SIGNIFICANCE

A Ferrous Steel Plate Coupler bar is an alternative solution to improve the existing details (replace standard 90-degree hook) as well as overall behavior of the specimen. The use of standard 90-degree hook causes many construction difficulties such as fabrication, fixing, (installation), compaction of concrete and steel congestion, increased manpower, increased time etc. Providing coupler in the joint region offers a good solution to encounter the above problem. To determine the shear capacity and overall performance of the Ferrous Steel Plate Coupler bar (SFCB) joint specimen, a reverse cyclic test was conducted on the interior joint with three categories of joint details (refer fig. All the specimen have been tested under displacement control mode with increasing drift ratio. The test results provide valuable interior joint constructed with Ferrous Steel Plate Coupler. Also, this study provides test observation, comparative analysis of joint shear stress with national and internal codes, comparison of shear strength with an existing model proposed by [5] and summary of all the observed results.

EXPERIMENTAL PROGRAMME

Materials

All the specimens have been cast with M20 grade of concrete and Fe500 grade of steel. The 53 grade of OPC cement has been used for casting the specimen. The river sand was used as fine aggregate and

crushed granite was used as coarse aggregate. The fineness modulus of fine and coarse aggregate was 2.63 and 6.83 respectively. The concrete mix M30 was designed as per IS code IS 10262:1992 and SP 23:1982. The designed mix proportion for M30 grade of concrete is 1:2.4:3:1 and Table 1 shows the weight of proportioned ingredients per meter cubic volume of concrete. To determine the compressive strength and modulus of elasticity of concrete a cube of 150 mm size was cast and tested. The average compressive strength and modulus of elasticity of concrete at the testing date was 47.90 N/mm² and 30.8 N/mm² respectively.

Table 1: Material property and Mix proportion

Fineness modulus	Fineness modulus	Cement (Kg/m ³)	FA*1 (Kg/m ³)	CA*2 (Kg/m ³)	Water (Kg/m ³)	W/c*3	(Kg/m ³)
FA*1	CA*2					Ratio	
2.63	6.83	330	170	850	1100	0.5	2.5
*1Fine aggregate; *2Coarse aggregate; *3Water cement ratio; *4Fineness modulus							

Specimen geometry

The test involves totally four sets of eight numbers of half scaled exterior specimen have been tested under seismic condition (reverse cyclic loading). The designation of test specimens is denoted as E-CMRJ, E-SMRJ, E-OMRJ and E-FTJ and all having a similar geometry and same material property. Table: 2 & 3 illustrates the schematic dimension and beam anchorage details of E-CMRJ, E-OMRJ, E-SMRJ and E-FTJ specimens. The length of the column and beam were 1500mm and 900mm respectively. The size of the beam was 125x175 and length of the beam was 900mm. The specimen detail was shown in the table 2.

Table 2: Test specimen details

Specim		E-CMRJ	E-SMRJ	E-OMRJ	E-FTJ
--------	--	--------	--------	--------	-------

en ID					
Joint details (mm)	f'c (MPA)	47.74	48.13	47.39	48.3
Column details (mm)	Length	1500	1500	1500	1500
	Breadth	125	125	125	125
	Depth	175	175	175	175
	Main rei.	4Nos-10	4Nos-10	4Nos-10	4Nos-10
	Shear rei.	6Ø@125mm c/c	6Ø@125mm c/c	6Ø@125mm c/c	6Ø@125mm c/c
Beam details (mm)	Length	900	900	900	900
	Breadth	175	175	175	175
	Depth	125	125	125	125
	Main rei.	4Nos-10	4Nos-10	4Nos-10	4Nos-10
	Shear rei.	6Ø@110mm c/c	6Ø@110mm c/c	6Ø@110mm c/c	6Ø@110mm c/c
<p>*1 Two legged stirrups Ø 6 @75mm c/c for a distance of 490 mm at either side of the column and remaining portion 100mm c/c</p> <p>*2 Two legged stirrups Ø 6 @35mm c/c for a distance of 310mm from the face of the column and remaining portion 70mm c/c</p>					

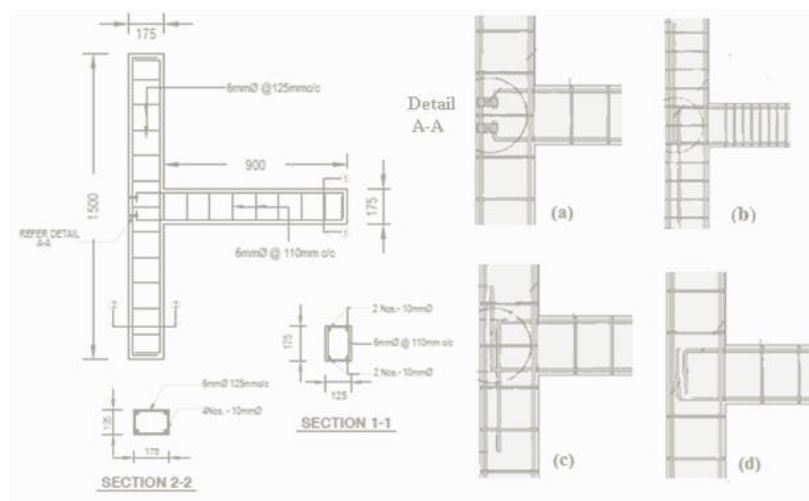


Figure 1: Joint details (a) Proposed coupler joint case 1, case 2, case 3, and case 4

Test programme

Fig. 2&3(a) illustrate the experimental load setup for an interior joint. The loading setup consists of gravity and lateral loading system. A 40kN gravity load (column axial load) was applied by means of 50 Tonne capacity hydraulic jack. This column axial is common for the entire test specimen. The lateral load was applied by means of 3 Tonne capacity push-pull jack and it is applied at end of the beam (refer fig. 2 (a)) at the end of the beam tip. The reverse cyclic load (lateral load) application was performed under displacement control method with the predetermined drift ratio and reverse cyclic loading was followed as per the loading protocol recommended by ACI T1.1R-01.

TABLE 3. BEAM MAIN BAR ANCHORAGE AND DEVELOPMENT LENGTH DETAILS

Specimen ID	Grade of Concrete & Reinf.	Code Details	Development	Length (mm)	Anchorage type
E-CMRJ		-	-		Coupler anchor
E-SMRJ	M20 & Fe 500	IS13929-1993	Tension side	625	90 degree
			: Compression sides:	625	Standard bent anchorage
E-OMRJ		IS456-2000	Tension side	565	90 degree
			: Compression	465	Standard bent anchorage

		sides:			
E-FTJ	-		-	-	No anchorage

Fig. 2 (b) shows the loading step and the number of cycles for each drift specified in the ACI Protocol. The loading history is based on the storey drift and each drift consist of three full reverse cycle loading. Table 3 illustrates about the beam main bar anchorage. During the test totally three categories of the output were measured that is a force, joint rotation and strain. The force and strain were recorded through the data acquisition system. LVDT was used to measure joint rotation and linear deformation at different locations. The steel strain was measured locally on the reinforcement by means of foil type strain gauge and the concrete strain was measured using Demec gauge instrument.

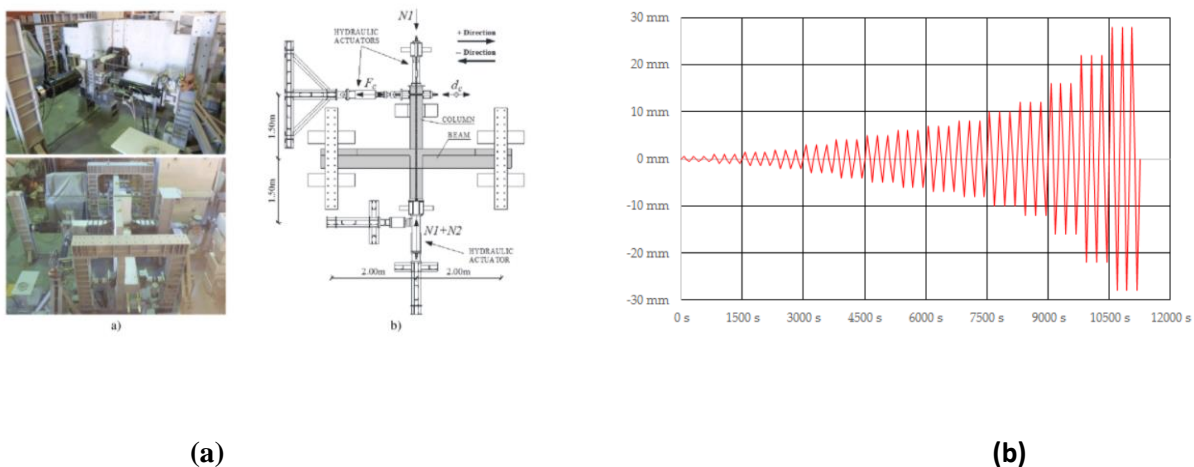


Figure 2: (a) Experimental test set up for interior joint (b) Reverse cyclic loading protocol

BEHAVIOUR OF SPECIMEN

Ultimate load

To determine the overall behavior of the test specimen the hysteresis loops were replotted. It is obtained by plotting the horizontal load versus horizontal displacement. These loops indicate information about the cracking of concrete and yielding steel due to cyclic loading. Table .4 & Fig.3(b) shows the

ultimate load carrying capacity for all the four groups of specimen and Fig. 5(a) illustrate the load envelop curve of hysteresis loops for the entire group's specimen. From this curve, the load carrying capacity, yield displacement, ultimate displacement and ductility of the specimens were obtained and listed in Table. 4. From the table 4, it is observed that the average load carrying capacity of CASE 1, E- SMRJ, CASE 3 and CASE 4 specimens' were 18.38 kN, 19.53kN, 18.40kN and 17.65kN and corresponding displacement were found 48, 49, 45 and 42mm displacement. From table 4, it is found that the ultimate load of CASE 2 specimen was 12% higher than that of CASE 1 specimen and performed better in resisting the load. This improvement in CASE 2 was mainly due to the presence of higher amount stirrups in the beam, column and joint region and the main bar were anchored with large development length in the core joint. (refer Fig.1 (b)). The ultimate load carrying of CASE 1 and CASE 3 specimen was almost equal performance in resisting the load. This may be due to the detailing of reinforcement were the same except joint detail that is the method of anchorage was different (refer fig.1 (a) & (c)). Similarly, the ultimate load carrying capacity of CASE 4 is 10% lower than the CASE 1. The main reason for lowering the strength is mainly due to the lack of anchorage that is proper anchorage. Table 4 illustrate the details of the initial crack load, average ultimate load carrying capacity of the CASE 1, CASE 2, CASE 3 and CASE 4 specimens.

Table 4: Observed initial crack load and average ultimate load

Test Specimen ID	Initial Crack load (kN)	Pu*1 (+)ve (kN)	Pu (-)ve (kN)	Pu (Average)	Mu*2 (kN)	Mu limit* 3 (kN)	Mu/Mu limit
CASE 1	13.00	18.41	18.36	18.38	15.6	17.10	0.91
CASE 2	8.50	19.46	19.60	19.53	16.6	16.62	1.00
CASE 3	6.60	18.41	18.40	18.40	15.64	17.41	0.90
CASE 4	6.60	17.6	17.71	17.65	15.00	15.80	0.95

*1Ultimate load; *2 Moment resistance of beam; *3 Limiting moment of resistance of beam;

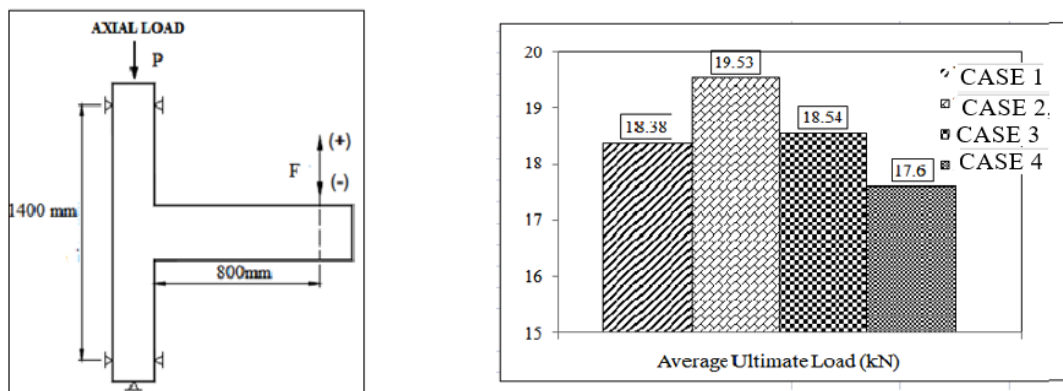


Figure 3: (a) Schematic diagram of loading set up (b) Ultimate load comparison for all group of specimen

Ductility

In an earthquake resistant structure, the ductility is the most important parameter to illustrate the level of safety. Good ductile structures are generally having the capacity of able to dissipate a significant amount of energy during cyclic deformations. The ductility of the specimen is expressed by the ductility factor (μ). The ductility of the specimen is defined as the ratio of ultimate deformation (Δ_{max}) to the corresponding deformation when yielding (Δ_y) occurs. i.e. $\mu = (\Delta_{max} / \Delta_y)$. Table .5 & Fig.4 (a) shows the ductility factor for all the four groups of the specimen. From table 5, it is found that the ductility factor

of CASE 1, CASE 2, CASE 3 and CASE 4 specimen are 17.5, 6.00, 4.67 and 4.11. The ductility factor is 2.9 times higher than CASE 2 specimen and 3.70 times higher than CASE 3 specimen and 4.25 times higher than CASE 4 specimen. So among all the specimens, the performance of the CASE 1 specimen is excellent than the other specimens. In the CASE 1 specimen during reverse cyclic loading a large deformation was found from 19mm cycle (refer fig.5 (a)) to till ending (48mm cycle) of the test without a reduction in the strength. Hence CASE 1 specimen is more ductile specimen and the load-envelope curve clearly indicates the ductile performance and the proposed coupler joint (CASE 1 specimens) are most beneficial in the seismic regions.

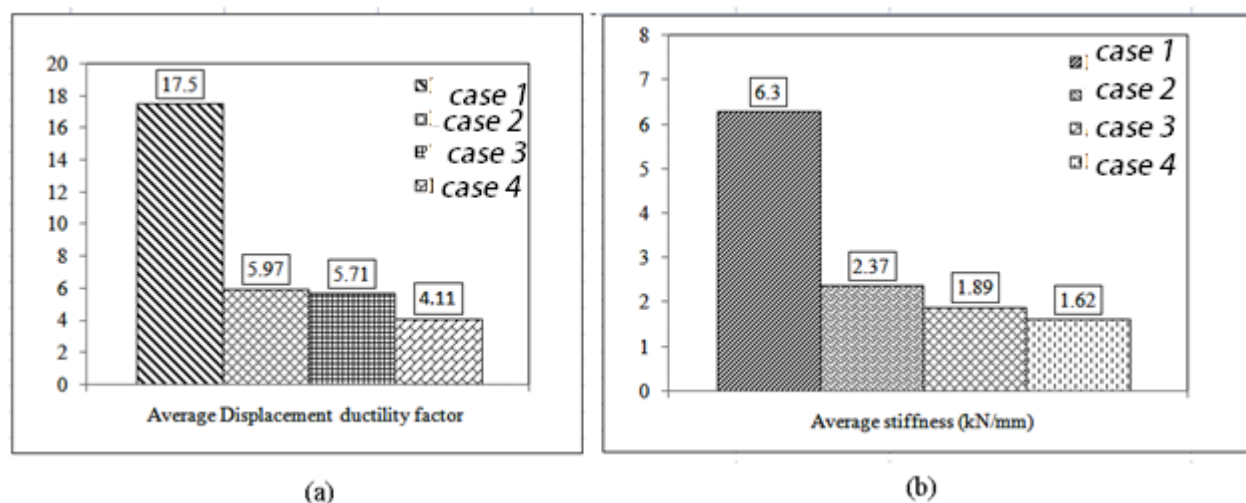


Figure 4: (a) Displacement ductility comparison for CASE 1, CASE 2, CASE 2, CASE 4 specimen (b) Average stiffness comparison for CASE 1, CASE 2, CASE 2, CASE 4 specimen.

Table 5: Observed Ultimate load carrying capacity of the specimens

Specimen Id	Yield displacement		Ultimate displacement		Average displacement Ductility factor	Average Stiffness (kN/mm)
	(Δy) (+)ve*1	(mm) (-ve*2)	(Δ_{max}) (+)ve*1	(mm) (-ve*2)		
CASE 1	3.20	2.40	48	48	7.00	6.33
CASE 2	11.6	6.40	48	50	6.00	4.73
CASE 3	11.6	8.40	42	48	4.60	1.88
CASE 4	5.6	10.8	42	42	4.10	1.62

*1(+ve): Positive direction *2(-ve): Negative direction

Stiffness

Table .5 & Fig. 5(b) illustrate the stiffness behavior for CASE 1, CASE 2, CASE 2, CASE 4 specimen. The stiffness is defined as the required load for the unit deformation of the joint. During the

reversal loading, micro cracks are initiated inside the joint. This formation cracks are interrupting force flow between the reinforcement and concrete and finally, the crack reduces the strength and will increase the deformation which may consequently reduce the stiffness. From the table 5, it is found that the stiffness value of CASE 1, CASE 2, CASE 3 and CASE 4 specimen are 6.33kN/mm, 2.36kN/mm, 1.88kN/mm and 1.62kN/mm. The stiffness factor for CASE 1 specimen is 2.7 times higher than CASE 2 specimen and 3.4 times higher than CASE 3 specimen and 3.9 times higher than CASE 4 specimen. So among all the specimens, the performance of the CASE 1 specimen is excellent than the other specimens. Also, from the graph 5, it is found that the stiffness degradation rate is similar for all group of the specimen (except initial stiffness) and the initial stiffness value is not the same for all the category of the specimen.

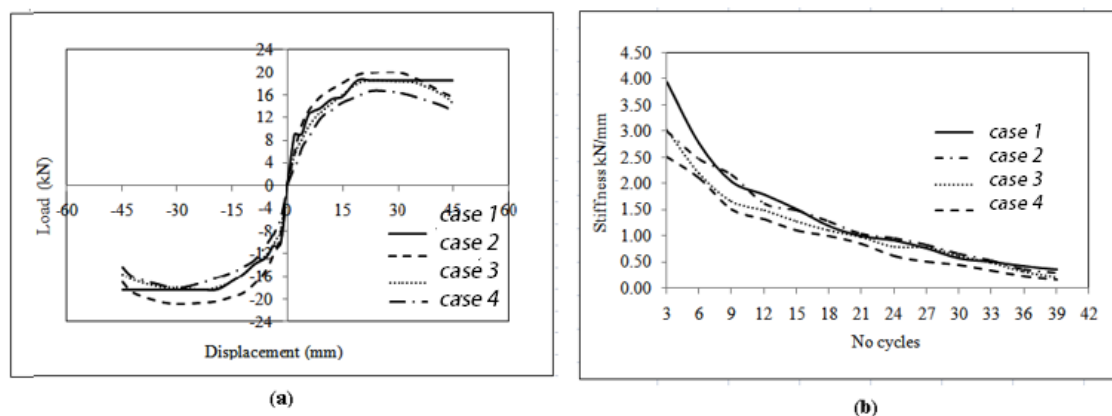


Figure 5: (a) Load-envelope curve for CASE 1, CASE 2, CASE 2, CASE 4 specimen (b)Comparative study of stiffness degradation for CASE 1, CASE 2, CASE 2, CASE 4 specimen.

Failure mode

Fig. 6 illustrates the failure pattern of CASE 1, CASE 2, CASE 3 and CASE 4 specimens. The development of crack which occurs at the end of each load cycle has been observed carefully and noted manually by marking the cracks. In the experiment, it was found that there are two types of cracks have been formed on the specimens and those are flexural cracks and shear cracks. From the experimental test, it is observed that initially, the entire specimen had the same kind of behavior was observed. The initial cracks (flexural cracks) in the beam appeared in CASE 1, CASE 2, CASE 3 and CASE 4 specimens were 9mm, 4mm and 3mm respectively and diagonal cracks were 19mm, 19mm and 12mm displacement respectively. Similarly "X" shaped cracks in the joint region were 42mm, 35mm, 30mm and plastic

hinge were developed at beams are 48mm, 42mm, 42mm displacement respectively. From the detailed observation, it is found that the initial crack developed at the beam in the CASE 1 was delayed and less damage was observed in the beam and joint region. Further, no plastic hinges are developed inside the joint in the CASE 1 specimen whereas in the E-FTJs specimen the plastic hinge was developed inside of the joint. Hence, it is concluded that the behavior of CASE 1 specimen is more effective in controlling the damages in the joint than that of CASE 2, CASE 3 and CASE 4 specimens.

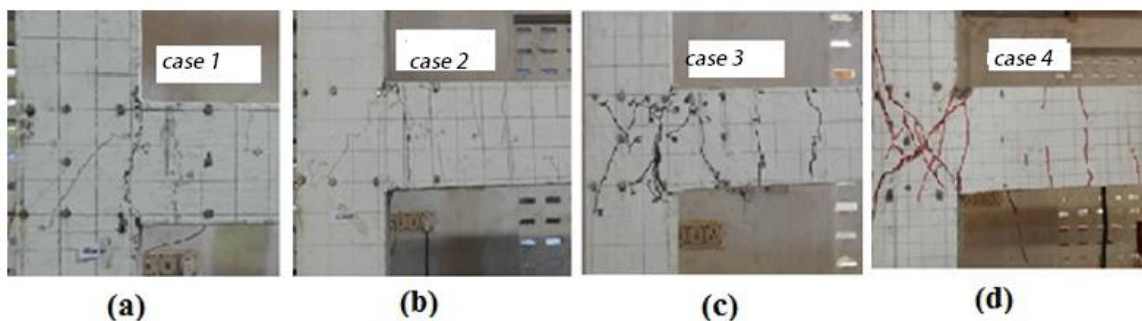


Figure 6: (a) Test specimen CASE 1 (b) Test specimen CASE 2 (c) Test specimen CASE 3 (d) Test specimen CASE 4 -Photographs for crack pattern of all specimens

JOINT CORE REQUIREMENTS FOR ANCHORAGE AND CONFINEMENT

The seismic behavior of joints generally depends on the shear mechanism (strut and truss mechanism), the grade of concrete, anchorage of beam longitudinal reinforcement in the core region and confinement in the form of a transverse beam or in the form of hoop reinforcement (either rectangular tie or spiral). In which anchorage type of beam's longitudinal bars and confinement of joint are most important and previous earthquake history reported that the RC building was suffered severe damage or collapse especially the interior joint had more affected than the interior joint. These failures were happened due to lack of knowledge of the above joint core requirement in the joint region.

Anchorage of beam main bar in the core of joint:

For resisting the seismic forces the quality of anchorage given to the beam main reinforcement in the joint is very important to ensure composite action between steel and concrete. Generally, it is achieved by a combination of bond and bearing on hooks. To avoid serious anchorage failure proper the joint of the member should have the proper design, detailing and code recommendation. The code IS 13920 & ACI 352-2 (2002) also strongly recommended the use of anchorage in the core joints region. For non-ductile joint, the development of length (L_d) is calculated as per clause 26.2 of IS 456-2000 code and for ductile detailing as per clause 6.2.5 of IS 13920-1993 code.

Confinement of core by transverse reinforcement:

The successful transmission of shear force in the joint can be achieved by providing adequate lateral confinement to the joint core. The effective confinement may be achieved by either by beams or by lateral ties/stirrups or by spiral hoops provided within the joint. The confinement by transverse reinforcement and transverse members are recommended in Section 4.2.1 and 4.2.2 of ACI 352R. For type 2 joint (ductile joint) the confinement of the joint by rectangular hoop reinforcement is calculated by the formula. The shear reinforcement for non-seismic region may be gravity load design (non-ductile joint) calculated as per 26.2.2.4 of IS 456-2000 and ductile detailing as per clause 6.3.5 of IS 13920-1993. The special confining reinforcement has been calculated as per clause 7.4 and 8 of IS 13920-1993.

EVALUATION OF THEORETICAL SHEAR STRENGTH FOR EXTERIOR JOINT

Shear strength of interior joint

The shear force (V_j) in the joint is computed by considering tension force in the beam main reinforcement (T) and shear force in the column (V_{col}). The expression for joint shear force V_j is

$$V_j = T - V_{col} \quad \text{---(10)}$$

The value of steel tension force (T) and column shear force (V_{col}) may be calculated by the following equation

Where ' P ' is the load applied in the beam; ' d_b ' is the effective depth of the beam; ' h_c ' is the depth of column; ' l_b ' is the length of the beam and ' l_c ' is the length of the column.

The shear stress in the joint depends on the shear area and the shear area is based on the dimension of beams and columns. The effective shear area (A_{core}^h) is calculated by multiplication

of width of the joint and depth of the joint. The horizontal shear stress (τ_{jh}) and vertical shear stress (τ_{jv}) may be calculated by the following equation.

Where 'H' is the shear force; ' A_{core}^h ' is Horizontal cross-sectional areas of the joint core; ' A_{core}^v ' is vertical cross-sectional areas of the joint core ' L_b ' is the length of the beam; ' d_b ' is effective depth of the beam; ' D_c ' is overall depth of the column; ' L_c ' is length of the column; ' D_b ' is overall depth of the beam;

Jointshearstress(HorizontalshearstressandVerticalshearstress)

Table 6 showing the estimated horizontal shear stress (τ_{jh}) and vertical shear stress (τ_{jv}) for all the specimen. The estimated horizontal and vertical shear stress is compared with different codes such as ACI, NZS, EN and IS 13920-1993 draft etc., The strength and stiffness of the joints most affected by joint shear stress and all the code gives an important for this. The shear capacity is based on the strut mechanism and all the codes follow the same mechanism. The strut mechanism generally depends on concrete strength and amount of hoop reinforcement in the core joint. The code ACI suggests $1.7(f'_c)0.5 A_j$ if confined on four sides $1.25(f'_c)0.5 A_j$ if the joint is confined on three sides and $1.7(f'_c)0.5 A_j$ for other cases. From the table. 6, it is observed that the code ACI 352-1991 suggested limiting shear stress for CASE 1, CASE 2, CASE 3 and CASE 4 is 5.65, 5.58, 5.7 and 5.44 MPa respectively. Similarly, The code NZS 3101; 1995 suggests limiting value of shear stress is $0.2(f'_c)$ and limiting shear stress for CASE 1, CASE 2, CASE 3 and CASE 4 is 6.4, 6.

Table 6. Horizontal (τ_{jh}) and Vertical shear (τ_{jv}) stress for interior joint

Specimen Id	rjh	rjv		Maximum as per ACI* 1 (1.0(f' _c)0.5)	Permissible as per NZS*2 (0.2(f' _c)0.5)	Shear stress as per EN*3 (1.1(f' _c)0.5)	(MPa) as per IS 13920*4 (1.1(f' _c)0.5)
	(MPa)	(MPa)	(MPa)				
E-CMRJ	32.02	5.21	3.13	5.65	6.4	9.26	6.22
E-SMRJ	31.12	5.54	3.32	5.58	6.22	9.04	6.13
E-OMRJ	32.60	5.22	3.13	5.70	6.52	9.39	6.28
E-FTJ	29.60	5.00	3.00	5.44	5.92	8.70	5.98

6.52 and 5.92 MPa respectively. The code EN 1998-1:2003 suggests limiting value of shear stress is $(1.1(f'_c)0.5)$ and limiting shear stress for CASE 1, CASE 2, CASE 3 and CASE 4 are 9.26, 9.04, 9.39 and 8.70 MPa respectively. Similarly, the code IS 13920-1993 draft suggests limiting value of shear

stress is $(1.1(f'_c)0.5)$ and limiting shear stress for CASE 1, CASE 2, CASE 3 and CASE 4 are 6.22, 6.13, 6.28 and 5.98MPa respectively. Among all the codes the ACI352-1991 gives very closer value and the code EN 1998-1:2003 gives a higher value than that of ACI352-1991. The fig. 7 & 8 shows a comparative study of horizontal shear stress (τ_{jh}) vs limiting shear stress recommended by different codes (ACI, NZS, EN and 13920-1993).

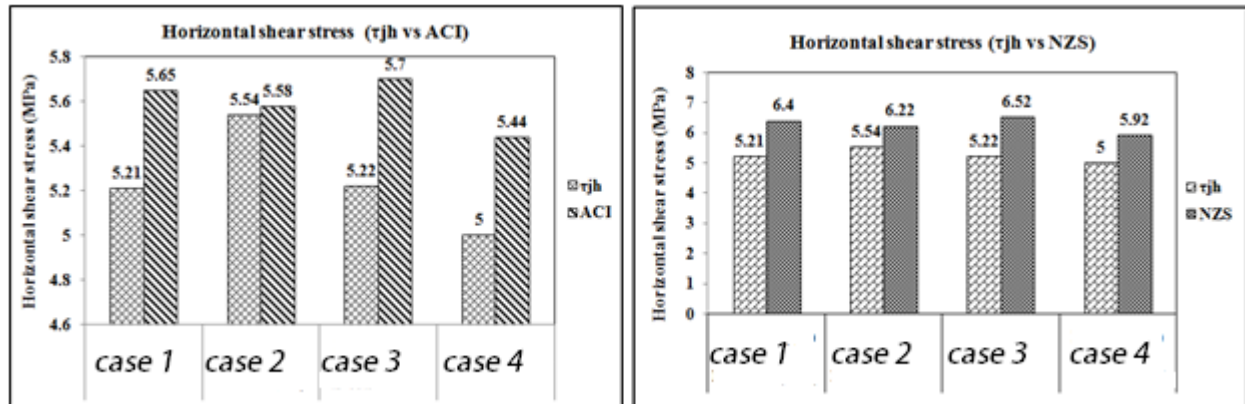


Figure 7: Comparison of Calculated Horizontal shear stress Vs Maximum Permissible shear stress (ACI & NZS)

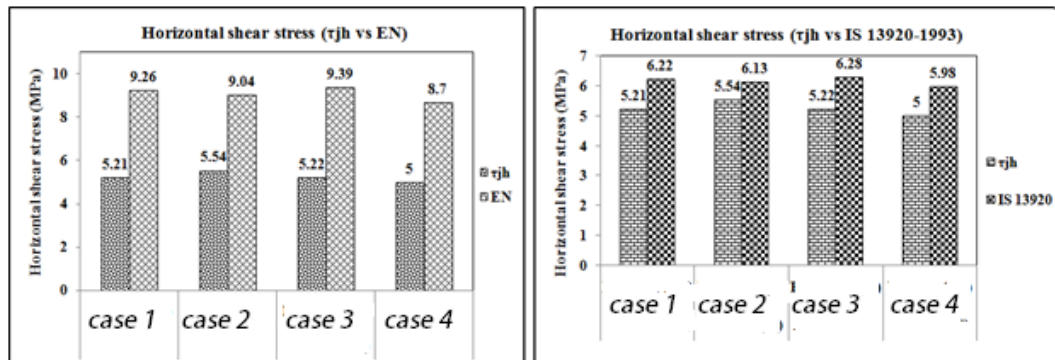


Figure 8: Comparison of Calculated horizontal shear stress Vs Maximum permissible shear stress (EN & IS 13920)

COMPARISON OF JOINT SHEAR STRENGTH WITH DESIGN CODES

Joint shear strength based on code ACI352-1991

The code ACI-352 (1992) recommended empirical equation for computing the nominal shear strength (V_n) of the interior joint is

$$\phi V_n = \phi Y(f'_c)^{0.5} A_j > V_j \quad \text{---(14)}$$

Where A_j is effective area of joint; ϕ is 0.85 (" ϕ " value is based on the effect of transverse beam), Y is the shear strength coefficient factor depends on types of joint. For exterior joint, Y is taken as 20 for Type 1 joint and 15 for Type 2 joint, $f'_c = 0.8f_{cu}$; f_{cu} = cylindrical compressive strength in MPa

5.1. Joint shear strength based on code NZS3101;1995

The code **NZS 3101;1995** recommended empirical equation for computing the nominal shear strength (V_n) of the interior joint is

$$V_n = 0.2(f'_c)^{0.5} A_j \quad \text{---(15)}$$

Where, $f'_c = 0.8f_{cu}$; f_{cu} = cylindrical compressive strength in MPa and A_j is effective area of joint and effective area may be calculated by multiplication of effective width of joint (b_j) and depth of the column(h).

Joint shear strength based on code EN1998-1:2003

The code EN 1998-1:2003 recommended empirical equation for computing the nominal shear strength (V_n) of the interior joint is

$$V_{jh} = \eta f_{cd} (1 - (v_d / \eta))^{0.5} A_j \quad \text{---(16)}$$

Where η is reduction factor on concrete compressive strength; f_{cd} is design value of compressive strength ; v_d is axial load in column ; A_j is effective area of joint

Joint shear strength based on code IS13920-1993

The code IS13920-1993 draft recommended empirical equation for computing the nominal shear strength (V_n) of the interior joint is

$V_n = 1.1(f'_c)^{0.5} A_j$ 'in the literature study, **Bakir (2003)** carried out a regression analysis and obtained regression statistics by using variables. The variables used for regression statistic analysis are concrete compressive strength, concrete cylinder strength, yield strength of stirrup, ratio of hoop reinforcement (stirrups), reinforcement ratio for column and beam, and ratio of height of column to the diameter of beam bars etc., Based on these studies, the **Bakir, (2003)** suggested the following equation for predicting the joint shear strength for interior joint .

Predicted shear strength proposed by Jihuru et al.(1992)

To represent the seismic behaviour of joint Jihuru et al. (1992) developed a model for predicting the ultimate shear strength of the RC interior joint. The model was developed based on the assumption that even after cracking, considerable tensile stress remains in the concrete until the fibres are pulled out from the matrix. The variables used for in this model are width and depth of the column, effective width and depth of joint, axial compressive load of column, compressive strength of concrete etc., The predicting the ultimate shear strength of the RC joints is calculated by summation of shear carried by the concrete (V_c), shear carried by fibre (V_f) (in this case V_f is zero and no fibre has been added in the concrete) and shear carried by the joint stirrups (V_s). The empirical equation for calculating the ultimate shear strength is

$$V = V_c + V_f + V_s \quad \text{---(19)}$$

Table 7 Comparative study of shear strength(Experimental vs theoretical model)

Specimen ID	T*1 (kN)	V _{col} *2 (kN)	V _j *3 (kN)	V _n *4 as per ACI	As per NZS	As per En	As per 13920	Theoretical strength Bakir (2003)	Shear (kN) Jihuru (1992)
E-CMRJ	108.29	12.76	95.72	123.29	140.00	202.36	136.02	66.17	75.76
E-SMRJ	115.28	13.56	101.71	121.54	136.00	197.75	134.09	64.29	72.20
E-OMRJ	108.61	12.77	95.83	124.39	142.62	205.41	137.37	67.35	76.75
E-FTJ	104.18	12.25	91.92	118.53	129.5	190.31	130.81	61.46	68.55

*1 Steel Tensile force; *2 Column shear force; *3 Joint shear force; *4 Nominal shear strength

The Table 7 shows shear strength based on code recommendation and experimental shear strength for various types of joints. From the table 7, it is observed that the shear strength calculated based on the code recommended values are higher than that of experimental value for all the specimen. Similarly, the theoretical strength calculated by Bakir (2003) and Jihuru (1992) model equation is lower than that of nominal and experimental shear strength. The fig. 9 shows a comparative graph for experimental shear strength and predicting shear strength using Bakir (2003) & Jihuru (1992) model equation. The ratio of experimental and theoretical shear strength calculated by Bakir

(2003) model for CASE 1, CASE 2, E- OMRJ and CASE 4 is 1.45, 1.58, 1.42, 1.50 respectively. Similarly, the ratio of experimental and theoretical shear strength calculated by Jihuru (1992) model for CASE 1, CASE 2, CASE 3 and CASE 4 is 1.26, 1.40, 1.25, 1.34 respectively. The shear strength calculated by JihurumodelisclosetoexperimentalsshearstrengthvaluethanthatofBakirmodel.

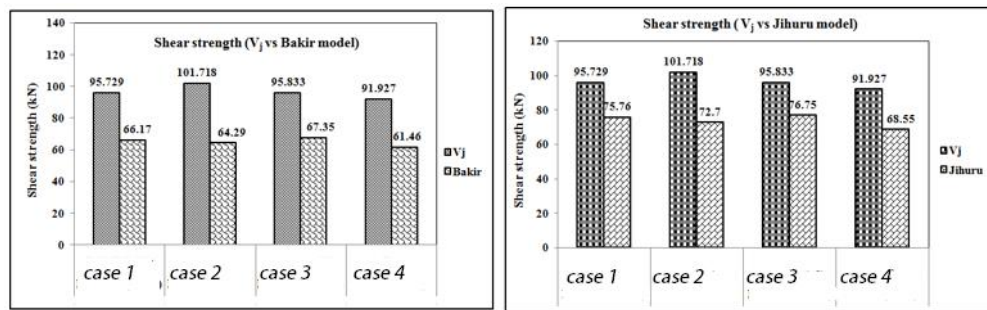


Figure 9: Comparison of experimental shear strength Vs Theoretical model shear strength (Bakir and Jihuru)

RESULTS AND DISCUSSION

An experimental and theoretical study on RC Interior joint has been performed under seismic loading condition. To find the effectiveness of the proposed Ferrous Steel Plate Coupler joint case 1, three different category joints detailing (CASE 2, CASE 3 and CASE 4) have been chosen and these specimens were tested by reverse cyclic loading. The experimental shear strength of all the tested specimens was compared with international code and national code. From the detailed experimental and theoretical study the following conclusions have been drawn

Conclusion drawn from the experiment

From the experimental and theoretical study, it is observed that the proposed steel flat coupler joint specimen is capable of resisting shear force under seismic loading condition. From the ductile point of view, the proposed Ferrous Steel Plate Coupler joint specimen was performed better than that of the other specimens. The displacement ductility factor for the proposed coupler joint specimen case 1 was 2.9 times higher than E-SMRJ specimen and 3.7 times higher than CASE 3 specimen. 4.25 times higher than CASE 4 specimen. The initial flexural crack appeared in the beam at 9mm displacement cycle in CASE 1 specimen whereas it appeared at 6mm displacement cycle in E-SMRJ specimen and 3mm displacement cycle in E-OMRJ specimen. When comparing all other specimens the initial crack has been delayed in the proposed Ferrous Steel Plate Coupler joint specimen. This behavior of the specimen indicated that the initial stiffness of the specimen directly increased. The

initial stiffness for E-CMRJ specimen was 2.67 times higher than E-SMRJ specimen and 3.36 times higher than E-OMRJ specimen. 3.90 times higher than E-FTJ specimen. The cracks appeared in the proposed Ferrous Steel Plate Coupler joint specimen (E-CMRJ) was found to be very less than the E-SMRJ, E-OMRJ and E-FTJ specimen. Further, the initial crack developed at the beam in the E-CMRJ specimen was delayed and less joint damage was observed in the beam and joint region. Hence, it is concluded that the performance of E-CMRJ specimen is more effective in controlling the damages in the joint than all others specimens. The proposed joint technique was successfully eliminating the shear mode of failure and also it eliminates the cleavage fracture and pulls out the failure of the joint. Also, the test results indicate that the proposed joint specimen is a very effective method than that of specimen detailed by standard ninety-degree hook. No plastic hinges were developed inside the joint in the E-CMRJ specimen whereas in the E-FTJ specimen the plastic hinge was developed inside of the joint. From the cost and time point of view, the proposed techniques were found to be very effective and main important features of the proposed techniques are an easy installation, less time and usage of labor, manpower and machinery is comparatively very less than that of others specimens. The ratio of experimental and predicted shear strength calculated by Jihuru (1992) model for E-CMRJ, E-SMRJ, E-OMRJ and E-FTJ is 1.26, 1.40, 1.25, 1.34 respectively and these values are very close to experimental shear strength value than that of Bakir model (2003). The nominal shear strength calculated by the code ACI 352-1991 gives very close value to experimental shear strength than that of all other codes. Similarly, the nominal shear strength calculated by the code EN 1998-1:2003 gives a higher value than that of all other codes. The horizontal and vertical shear stress values for all specimen is lower than that of limiting value recommended by different codes such as ACI 352-1991, NZS 3101-1995, EN 1998-1:2003, IS 13920-1993 draft.

Reference

1. Mostofinejad, D., & Hajrasouliha, M. (2018). Shear retrofitting of corner 3D-reinforced concrete beam-column joints using externally bonded CFRP reinforcement on grooves. *Journal of Composites for Construction*, 22(5), 4018037.
2. Attari, N., Youcef, Y. S., & Amziane, S. (2019). Seismic performance of reinforced concrete beam--column joint strengthening by frp sheets. *Structures*, 20, 353–364.
3. Oinam, R. M., Kumar, P. C., & Sahoo, D. R. (2019). Cyclic performance of steel fiber-reinforced concrete exterior beam-column joints. *Earthquakes and Structures*, 16(5), 533–546.

4. Mostofinejad, D., & Akhlaghi, A. (2017). Experimental investigation of the efficacy of EBROG method in seismic rehabilitation of deficient reinforced concrete beam--column joints using CFRP sheets. *Journal of Composites for Construction*, 21(4), 4016116.
5. Halahla, A. M., Tahnat, Y. B. A., Almasri, A. H., & Voyiadjis, G. Z. (2019). The effect of shape memory alloys on the ductility of exterior reinforced concrete beam-column joints using the damage plasticity model. *Engineering Structures*, 200, 109676.
6. Marimuthu, K., & Kothandaraman, S. (n.d.). REVIEW ON THE METHODS OF REINFORCEMENT TECHNIQUE IN REINFORCED CONCRETE BEAM-COLUMN JOINT.
7. Mahmud, K., Town, G. E., Morsalin, S., & Hossain, M. J. (2018). Integration of electric vehicles and management in the internet of energy. *Renewable and Sustainable Energy Reviews*, 82, 4179–4203.
8. Foorginezhad, S., Mohseni-Dargah, M., Firoozirad, K., Aryai, V., Razmjou, A., Abbassi, R., Garaniya, V., Beheshti, A., & Asadnia, M. (2020). Recent advances in sensing and assessment of corrosion in sewage pipelines. *Process Safety and Environmental Protection*.
9. Tingjin, L., Lu, J., Wang, D., & Liu, H. (2021). Experimental Investigation of the Mechanical Behaviour of Wall--Beam--Strut Joints for Prefabricated Underground Construction. *International Journal of Concrete Structures and Materials*, 15(1).
10. Chetchotisak, P., Arjsri, E., & Teerawong, J. (2020). Strut-and-tie model for shear strength prediction of RC exterior beam--column joints under seismic loading. *Bulletin of Earthquake Engineering*, 18(4), 1525–1546.
11. Annadurai, A., & Ravichandran, A. (2018). Seismic Behavior of Beam--Column Joint Using Hybrid Fiber Reinforced High-Strength Concrete. *Iranian Journal of Science and Technology, Transactions of Civil Engineering*, 42(3), 275–286.
12. Wang, J. H. (2021). Cyclic behaviors of reinforced concrete beam-column joints with debonded reinforcements and beam failure: experiment and analysis. *Bulletin of Earthquake Engineering*, 19(1), 101–133.
13. Pantelides, C. P., Hansen, J., Ameli, M. J., & Reaveley, L. D. (2017). Seismic performance of reinforced concrete building exterior joints with substandard details. *Journal of Structural Integrity and Maintenance*, 2(1), 1–11.
14. Abdelwahed, B. (2019). Beam-Column Joints Reinforcement Detailing Adequacy in Case of a Corner Column Loss-Numerical Analysis. *Latin American Journal of Solids and Structures*, 16(7).
15. Mostofinejad, D., & Akhlaghi, A. (2017). Flexural strengthening of reinforced concrete beam-column joints using innovative anchorage system. *ACI Structural Journal*, 114(6), 1603–1614.

16. Hwang, H.-J., & Park, H.-G. (2020). Performance-based shear design of exterior beam-column joints with standard hooked bars. *ACI Structural Journal*, 117(2), 67–80.
17. Tran, C. T. N., & Li, B. (2020). Analytical model for shear-critical reinforced concrete interior beam-column joints. *Journal of Earthquake Engineering*, 24(8), 1205–1221.
18. Pauletta, M., Di Marco, C., Frappa, G., Somma, G., Pitacco, I., Miani, M., Das, S., & Russo, G. (2020). Semi-empirical model for shear strength of RC interior beam-column joints subjected to cyclic loads. *Engineering Structures*, 224, 111223.
19. Asha, P., and R. Sundararajan. "Effect of confinement on the seismic performance of reinforced concrete exterior beam-column joints." *Australian Journal of Structural Engineering* 19.1 (2018): 59-66.
20. Okeola, Abass Abayomi, John Mwero, and Abdulhafeez Bello. "Behavior of sisal fiber-reinforced concrete in exterior beam-column joint under monotonic loading." *Asian Journal of Civil Engineering* 22.4 (2021): 627-636.
21. Kalaivani, V., et al. "INVESTIGATION ON BEHAVIOUR OF EXTERIOR BEAM-COLUMN JOINT UNDER CYCLIC LOADING." *Pak. J. Biotechnol.* Vol 14.3 (2017): 449-452.
22. Rajeev, Anupoju, et al. "Experimental and numerical investigation of an exterior reinforced concrete beam-column joint subjected to shock loading." *International Journal of Impact Engineering* 137 (2020): 103473.
23. Maher, Mahmoud R., and Ashkan Torabi. "Retrofitting external RC beam-column joints of an ordinary MRF through plastic hinge relocation using FRP laminates." *Structures*. Vol. 22. Elsevier, 2019.
24. Adibi, Mahdi, Mohammad S. Marefat, and Reza Allahvirdizadeh. "Nonlinear modeling of cyclic response of RC beam-column joints reinforced by plain bars." *Bulletin of Earthquake Engineering* 16.11 (2018): 5529-5556.
25. Vandana, R. K., and K. R. Bindhu. "Influence of geometric and material characteristics on the behavior of reinforced concrete beam-column connections." *Canadian Journal of Civil Engineering* 44.5 (2017): 377-386.